Supplementary Information

Reconfiguration of Functional Brain Hierarchy in Schizophrenia

Irene Acero-Pousa[1,*], Anira Escrichs[1], Paulina Clara Dagnino[1], Yonatan Sanz Perl[1,2], Morten L. Kringelbach[3,4,5], Peter J. Uhlhass[6,7], Gustavo Deco[1,8,*]

Supplementary Methods

Whole-brain model

The whole-brain dynamics are represented by coupling the local dynamics of $N = 80$ Hopf-oscillators through the connectivity matrix C, which is given by:

$$\frac{dz_j}{dt} = \left(a_j + i\omega_j\right)z_j - \left|z_j\right|^2 z_j + \sum_{k=1}^{N} C_{jk}\left(z_k - z_j\right) + \eta_j \quad (1)$$

In this equation, $z_j = x_j + iy_j$ represents a complex state variable of region j where $x_j = Real\left(Z_j\right)$ and y_j is the imaginary part. η_j is the additive uncorrelated Gaussian noise with variance σ^2. The parameter a_j represents the node's bifurcation parameter, with $a_j < 0$ describing the local dynamics as a stable fixed point at $z = 0$ and $a_j > 0$ creating a stable limit cycle oscillation with frequency $f_j = \frac{w_j}{2}\pi$. The intrinsic node frequency w_j is obtained from the empirical data by averaging the peak frequency of each brain region. We selected the parameter $a = -0.02$ based on Deco et al (1), as it generates a signal that is more effective at preserving resting state network structure and dynamically responding brain networks. The proximity to this critical point holds significant importance as it facilitates linearity in the dynamics. This linearity enables an analytical solution for the connectivity matrix C, which is determined by computing Pearson correlations between each pair of brain regions. By employing a linear noise approximation (LNA) method, we can evaluate the functional correlations of the entire brain network. Consequently, the dynamical system involving N nodes (described by Equation 1) can be represented in a vectorized format:

$$\frac{dz}{dt} = (a - S + iw) \odot z - (z \odot \bar{z})z + Cz + \eta \quad (2)$$

Here, $z = \left[z_1,\ldots, z_N\right]^T$, $a = \left[a_1,\ldots, a_N\right]^T$, $w = \left[w_1,\ldots, w_N\right]^T$, $\eta = \left[\eta_1,\ldots, \eta_N\right]^T$, and $S = \left[S_1,\ldots, S_N\right]^T$, which is a vector indicating the connectivity strength of each node, where $S_i = \sum_j C_{ij}$. The transpose operation is denoted by $[\,]^T$, the $\odot$ symbol represents the element-wise multiplication, and z^- represents the complex conjugate of z. This equation describes the linear fluctuations around the fixed point $z = 0$, which is the solution of $\frac{dz}{dt} = 0$. The progression of the linear fluctuations can be articulated using a Langevin stochastic linear equation by segregating the real and imaginary components of the state variables and disregarding higher-order terms $(z \odot z^-)z$:

$$\frac{d}{dt}\delta u = J\delta u + \eta, \tag{3}$$

where the 2N-dimensional vector $\delta u = [\delta x, \delta y]^{\mathrm{T}} = [\delta x_1,\ldots, \delta x_N, \delta y_1,\ldots, \delta y_N]^{\mathrm{T}}$ includes the fluctuations in both the real and imaginary aspects of the state variables. The $2Nx2N$matrix J stands for the Jacobian of the system computed at the steady state and can be represented in the form of a block matrix:

$$J = \begin{bmatrix} Jxx & J_{xy} \\ J_{yx} & J_{yy} \end{bmatrix} \tag{4}$$

being $J_{xx}, J_{xy}, J_{yx}, J_{yy}$ matrices of size NxN. Specifically, $J_{xx} = J_{yy} = diag(a - S) + C$ and $J_{xy} = -J_{yx} = diag(w)$, where $diag(v)$ represents a diagonal matrix with the vector v on its diagonal. Importantly, this linearization is only applicable if $z = 0$ is a stable solution, meaning that all eigenvalues of J have a negative real part.

Model optimisation

In order to fit the model to the empirical data, we need to optimise the coupling matrix C, starting off the primer diffusion tensor imaging, such that the model accurately replicates the empirical covariances ($FC^{empirical}$), computed as the correlation matrix of the functional neuroimaging data, and the empirical time-shifted covariances ($FS^{empirical}(\tau)$), where τ denotes the time lag and are normalized by dividing each pair of nodes i,j by $\sqrt{KS_{ii}^{empirical}(0)KS_{jj}^{empirical}(0)}$. We select $\tau = 2$, which is the value that minimizes the average autocorrelation. Interestingly, adjusting the time-shifted correlations can introduce asymmetries in the coupling matrix C, leading to non-equilibrium dynamics and violations of the FDT. The fitting is performed using a heuristic pseudo-gradient approach, iterating by updating C until it is completely optimised using:

$$C_{ij} = C_{ij} + \alpha\left(FC_{ij}^{empirical} - FC_{ij}^{simulated}\right) + \varsigma\left(FS_{ij}^{empirical}(\tau) - FS_{ij}^{simulated}(\tau)\right) \quad (5)$$

To compute $FS_{ij}^{simulated}(\tau)$, we select the first N rows and columns of the simulated time-shifted covariances $KS^{simulated}(\tau)$ normalized by dividing each pair of nodes i,j by $\sqrt{KS_{ii}^{simulated}(0)KS_{jj}^{simulated}(0)}$. $KS^{simulated}(\tau)$ represents the simulated time-shifted covariance matrix and is calculated as:

$$KS^{simulated}(\tau) = exp(\tau J)K \quad (6)$$

In the fitting of the model, convergence is reached when the updated value of C reaches a stable value, indicating that the model is optimised. C is initialized using the anatomical connectivity and only updated if there are connections in this matrix. This is followed strictly except in the homologous connections between the same regions in

both hemispheres, which are also updated, as tractography is less accurate when incorporating this kind of connectivity. Moreover, α is set to 0.04 and ς is set to 0.01. For each iteration, we calculate the model results by evaluating the correspondence between simulated and empirical data. Specifically, we assess model fit using two metrics: (1) the Pearson correlation between the empirical and simulated functional connectivity matrices, and (2) the Pearson correlation between the empirical and simulated time-shifted covariance matrices. These correlations are computed over the lower triangle (excluding the diagonal) of each matrix. Finally, we refer to the optimised C as Effective Connectivity (EC) (2). Importantly, while the structural connectivity matrix C used as the baseline is symmetric, the iterative update procedure incorporates both symmetric functional connectivity and asymmetric time-shifted covariance matrices. The latter captures direction-dependent temporal relationships between brain regions, such that the covariance between region A and a time-lagged region B is not equal to the reverse. As a result, the model naturally evolves from a symmetric anatomical scaffold into a directed effective connectivity matrix, where asymmetry arises strictly from causal functional interactions rather than from structural architecture.

The median model fit between the simulated and empirical functional connectivity for subjects with schizophrenia was 0.64, while for controls, it was 0.72. On the other hand, the median fitting between the simulated and empirical covariance matrices was 0.60 for schizophrenia and 0.58 for controls. Statistical testing revealed a significant group difference for the functional connectivity fits ($p < 0.01$), while no significant difference was found for the time-shifted covariance fits ($p > 0.05$). Importantly, all subjects' fits exceeded the correlation between their empirical functional connectivity and structural connectivity, confirming the model's ability to capture meaningful functional dynamics.

References

1. Deco G, Kringelbach ML, Jirsa VK, Ritter P. The dynamics of resting fluctuations in the brain: metastability and its dynamical cortical core. Sci Rep. 2017;7(1):3095.
2. Kringelbach ML, Perl YS, Tagliazucchi E, Deco G. Toward naturalistic neuroscience: Mechanisms underlying the flattening of brain hierarchy in movie-watching compared to rest and task. Sci Adv. 2023;9(2):eade6049.

Supplementary Tables

RSN	FDT deviations in schizophrenia: median (IQR)	FDT deviations in controls: median (IQR)	Significance (p) after multiple comparisons correction
Visual	32.77 (31.01)	26.06 (30.51)	$p > 0.05$
Somatomotor	29.15 (17.89)	23.78 (15.49)	$p < 0.01$
Dorsal Attention	28.57 (31.99)	21.82 (20.81)	$p < 0.01$
Salience	34.73 (29.65)	29.80 (25.72	$p > 0.05$
Limbic	52.09 (39.48)	28.79 (38.33	$p< 0.001$
Control	39.14 (37.23)	23.26 (26.92)	$p < 0.01$
DMN	35.96 (38.51)	26.17 (26.98)	$p < 0.05$
Subcortical	43.77 (30.61)	29.84 (24.26)	$p < 0.01$

Supplementary Table 1: The hierarchical organisation is increased in some schizophrenia RSNs from the subject perspective. *This table presents the median and interquartile range (IQR) of the average FDT deviation values per subject in each group, categorized by RSNs. The significance column indicates the p-values obtained after correcting for múltiple comparisons*

RSN	FDT deviations in schizophrenia: median (IQR)	FDT deviations in controls: median (IQR)	Significance (p) after multiple comparisons correction
Visual	44.35 (17.15)	39.25 (4.73)	$p > 0.05$
Somatomotor	39.61 (5.84)	20.91 (10.37)	$p < 0.01$
Dorsal Attention	41.31 (3.16)	31.01 (0.95)	$p > 0.05$
Salience	44.60 (20.46)	33.51 (12.51)	$p < 0.05$
Limbic	57.86 (26.17)	44.37 (14.06)	$p < 0.05$
Control	48.91 (23.70)	30.97 (18.33)	$p > 0.05$
DMN	46.31 (7.73)	33.98 (3.39)	$p < 0.001$
Subcortical	53.17 (17.24)	37.05 (14.62)	$p < 0.15$

Supplementary Table 2: Increased hierarchical organisation in schizophrenia RSNs from the node perspective.. *This table indicates the median and interquartile range (IQR) of the average FDT deviation values per node in each group, categorized by RSNs. The significance column indicates the p-value obtained after correction for múltiple comparisons.*

RSN	FDT deviations in schizophrenia: mean (SD)	FDT deviations in controls: mean (SD)	Standardized mean difference between groups
Visual	45.19 (28.50)	39.04 (28.62)	0.21
Somatomotor	39.28 (30.00)	24.23 (10.03)	0.67
Dorsal Attention	41.31 (37.24)	31.01 (38.66)	0.27
Salience	48.03 (35.28)	34.89 (21.36)	0.45
Limbic	59.66 (32.35)	41.29 (31.52	0.57
Control	51.57 (39.17)	34.27 (27.41)	0.51
DMN	45.68 (30.87)	33.90 (21.51)	0.44
Subcortical	53.40 (28.93)	37.90 (22.14)	0.60

Supplementary Table 3: The hierarchical organisation is higher in all RSNs in schizophrenia. *This table indicates the mean and standard deviation (SD) of the average FDT deviation values per subject in each group, by RSNs. It also presents the standardized mean difference between the two groups, computed as the difference between the groups means divided by the pooled Standard deviation.*

Parameter name	Value
Bifurcation parameter (a)	-0.02
Noise variance (σ)	0.02
FC error multiplier (α)	0.04
COV error multiplier (ζ)	0,01
Tau	2

Supplementary Table 4: *Optimal parameters used for constructing the Hopf whole-brain model.*

Factor 1	Factor 2	Factor 3
left caudate (subcortical)	right medial orbitofrontal (limbic)	right medial orbitofrontal (limbic)
right parahippocampal (visual)	right entorhinal (limbic)	right entorhinal (limbic)
right thalamus (subcortical)	left medial orbitofrontal (limbic)	left medial orbitofrontal (limbic)
right transverse temporal (somatomotor)	left hippocampus (subcortical)	left lateral orbitofrontal (limbic)
left nucleus accumbens (subcortical)	left amygdala (subcortical)	left hippocampus (subcortical)

Supplementary Table 5: ***Each factor is characterised by specific brain areas.*** Brain areas showing the largest differences in hierarchical organization, with nodes exhibiting higher hierarchical values in the high-scoring group compared to the low-scoring group for each symptom factor. RSNs of the nodes are specified between parentheses.

Supplementary Figures

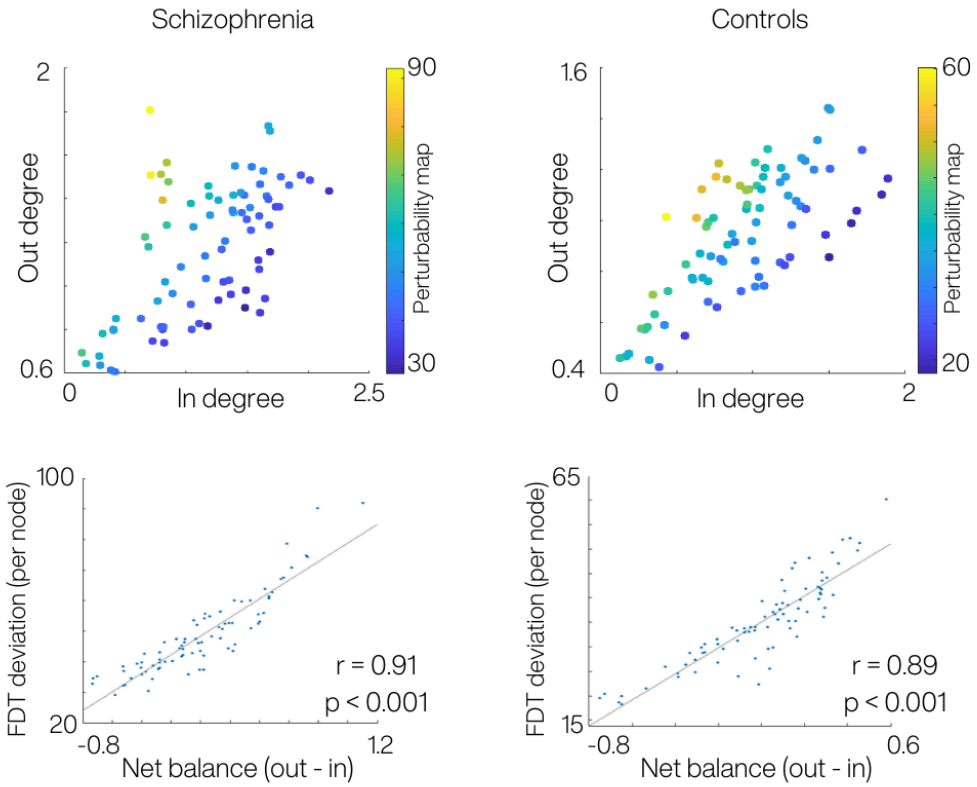

Supplementary Figure 1: Asymmetry between the out and in degree defines the FDT deviation and hierarchical position of a brain region. ***(a)*** *Nodes with higher FDT deviation tend to exhibit greater out-degree (number of outgoing connections) and lower in-degree (number of incoming connections), reflecting directional asymmetry in their influence over the network.* ***(b)*** *Nodes with higher net drive (out-degree minus in-degree) show stronger violations of the fluctuation-dissipation theorem (FDT), indicating greater departure from equilibrium dynamics. In our framework, this increased directional influence is interpreted as a signature of higher hierarchical position within the brain's functional architecture.*

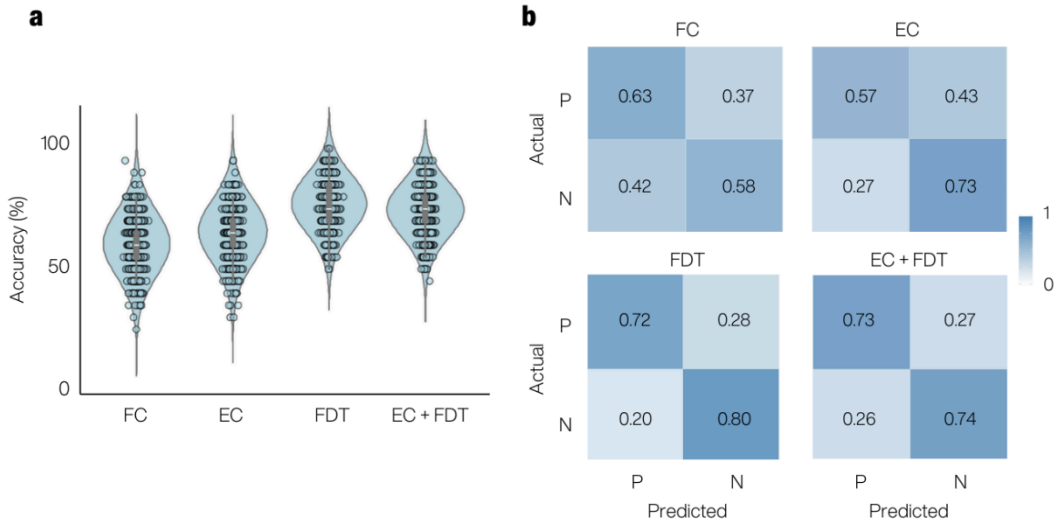

Supplementary Figure 2: Support Vector Machine classification achieves higher accuracy when hierarchical organization features are included. *Comparison of the accuracy obtained using a SVM algorithm with different inputs (FC, EC, FDT and EC+FDT) to identify the most informative metrics. a) Violin plots display the distribution of SVM accuracy across 1000 k-folds using FC, EC, FDT and EC + FDT data as inputs. To ensure same input dimensionality, a PCA was performed and only the first principal component was included in the SVM. b) Confusion matrices illustrate the overall accuracy achieved corresponding to the distributions in (a), presented as percentages represented on a color scale. P stands for positive, N for negative.*

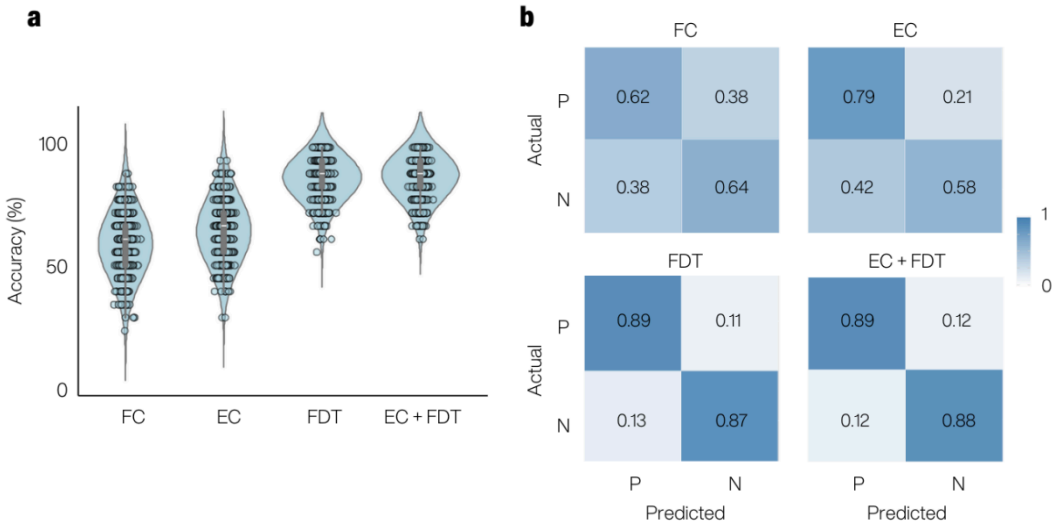

Supplementary Figure 3: Compared to dynamic functional or effective connectivity features, dynamic hierarchical organization features lead to improved accuracy in Support Vector Machine classification. *A sliding-window approach was used to capture the temporal dynamics of each metric (window size = 50 timepoints, overlap = 25). Within each window, FC was computed, and whole-brain models were estimated to extract EC and FDT deviations. These dynamic profiles were used as inputs to the SVM. To ensure same input dimensionality, a PCA was performed and only the first 10 principal components were included in the SVM. a) Violin plots display the distribution of SVM accuracy across 1000 k-folds using FC, EC, FDT and EC + FDT data as inputs. b) Confusion matrices illustrate the overall accuracy achieved corresponding to the distributions in (a), presented as percentages represented on a color scale. P stands for positive, N for negative.*